Molecular Crystals and Liquid Crystals

Publication details, including instructions for authors and subscription information:
http://www.tandfonline.com/loi/gmcl20

Structural, Optical, and Electrical Properties of One-Dimensional Bis(Dimethylglyoximato)nickel(II), $Ni(dmg)_2$ at High Pressure

K. Takeda [a] , J. Hayashi [a] , I. Shirotani [a] , H. Fukuda [a] & K. Yakushi [b]

[a] Muroran Institute of Technology, Mizumoto, Muroran-shi, Japan

[b] Institute for Molecular Science, Myodaiji, Okazaki-shi, Japan

Version of record first published: 20 Dec 2006

To cite this article: K. Takeda, J. Hayashi, I. Shirotani, H. Fukuda & K. Yakushi (2006): Structural, Optical, and Electrical Properties of One-Dimensional Bis(Dimethylglyoximato)nickel(II), $Ni(dmg)_2$ at High Pressure, Molecular Crystals and Liquid Crystals, 460:1, 131-144

To link to this article: http://dx.doi.org/10.1080/15421400600598412

Mol. Cryst. Liq. Cryst., Vol. 460, pp. 131–144, 2006

ISSN: 1542-1406 print/1563-5287 online
DOI: 10.1080/15421400600598412

Taylor & Francis
Taylor & Francis Group

Structural, Optical, and Electrical Properties of One-Dimensional Bis(Dimethylglyoximato)nickel(II), $Ni(dmg)_2$ at High Pressure

K. Takeda
J. Hayashi
I. Shirotani
H. Fukuda
Muroran Institute of Technology, Mizumoto, Muroran-shi, Japan

K. Yakushi
Institute for Molecular Science, Myodaiji, Okazaki-shi, Japan

By use of synchrotron radiation, powder X-ray diffraction of one-dimensional bis(dimethylglyoximato)nickel(II), $Ni(dmg)_2$, has been studied at room temperature and at high pressure. The lattice constants with an orthorhombic structure for $Ni(dmg)_2$ monotonically decrease with increasing pressure up to 7.4 GPa; the linear compressibility of each axis is estimated. The magnitude of the linear compressibility increases in the order $c > b > a$ in the low-pressure region. However, the lattice constant along the b-axis is smaller than that along the a-axis at pressures greater than 6 GPa. A Ni–Ni distance along the c-axis abruptly decreases from 3.255 Å at ambient pressure to 2.82 Å at 7.4 GPa. A bulk modulus of $Ni(dmg)_2$ is obtained from the volume versus pressure curve fitted by a Birch equation of state. The bulk modulus of this complex is very small, 8.0 GPa. $Ni(dmg)_2$ is a very compressible compound. The electrical and optical properties of $Ni(dmg)_2$ have been investigated at high pressures. The $d\pi$–π^* and 3d–4p bands shift to a lower energy region with increasing pressure. The absorption peak of the 3d–4p band is very sensitive to pressure. The resistivity of $Ni(dmg)_2$ decreases monotonically with increasing pressure up to 23 GPa. The lowest resistivity of this complex is about 50 Ω cm at around 23 GPa. These electrical and optical properties are closely related to the rapid shrinkage of the Ni–Ni distance with increasing pressure.

Keywords: bis(dimethylglyoximato)nickel(II); electrical and optical properties; high pressure; synchrotron radiation; X-ray diffraction

Address correspondence to I. Shirotani, Muroran Institute of Technology, 27-1, Mizumoto, Muroran-shi 050-8585, Japan. E-mail: sirotani@mmm.muroran-it.ac.jp

INTRODUCTION

Interesting electrical and optical behaviors of one-dimensional d^8-metal(II) complexes with dionedioxime ligands have been observed at high pressures [1–4]. The electrical resistivity of one-dimensional bis(dimethylglyoximato)platinum(II), $Pt(dmg)_2$, drastically decreases with increasing pressure, reaches the minimum at around 6.5 GPa, and then slowly increases with increasing pressure greater than this pressure. The insulator-to-metal-to-insulator (IMI) transitions for this complex occur at high pressures [1,2]. The similar transitions for bis(1,2-benzoquinonedioximato)platinum(II), $Pt(bqd)_2$, are also observed at around 0.8 GPa [3,4].

By use of synchrotron radiation, powder X-ray diffraction of several one-dimensional metal complexes has been studied at high pressures. The Pt–Pt distance along the one-dimensional chain for $Pt(dmg)_2$ decreases rapidly with increasing pressure. The one-dimensional bis (diphenylglyoximato)metal(II), $Pt(dpg)_2$, has the smallest bulk modulus [5]. The anomalous behavior for $Pt(bqd)_2$ has been found in lattice constant versus pressure curves at room temperature [6]. The pressure-induced amorphization and the solid-phase reaction occurs in the one-dimensional Pd complex, α-$Pd(bqd)_2$ [7].

A crystal structure of one-dimensional bis(dimethylglyoximato) nickel(II), $Ni(dmg)_2$, is orthorhombic, has space group I_{bam} [8], and is exhibited in Fig. 1. $Ni(dmg)_2$ is isostructural with $Pt(dmg)_2$. The complex crystallizes in linear chain columnar structures. The columns are formed by square planar complex molecules with a Ni–Ni distance of 3.255 Å in the direction of the stack [8]. The resistivity of $Ni(dmg)_2$ abruptly decreases with increasing pressure; however, the insulator-to-metal transition is not found up to 23 GPa [9]. An absorption spectrum of $Ni(dmg)_2$ comprises two bands at around 410 and 530 nm in the visible region at ambient pressure; the former band is ascribed to the metal-to-ligand charge transfer ($d\pi$–π^*) transition; latter band is assigned to the $3d_z^2$–$4p_z$ transition [10]. The d–p band of $Ni(dmg)_2$ rapidly shifts to the longer wavelength region with increasing pressure [11,12].

Using synchrotron radiation, we have studied powder X-ray diffraction of $Ni(dmg)_2$ up to 7.4 GPa at room temperature. Further, the absorption spectra and electrical resistivities of $Ni(dmg)_2$ have been studied in detail at high pressures. In this report, the relationship between the structure and physical properties in this complex is discussed. Further, the physical properties of $Ni(dmg)_2$ are compared to those of $Pt(dmg)_2$.

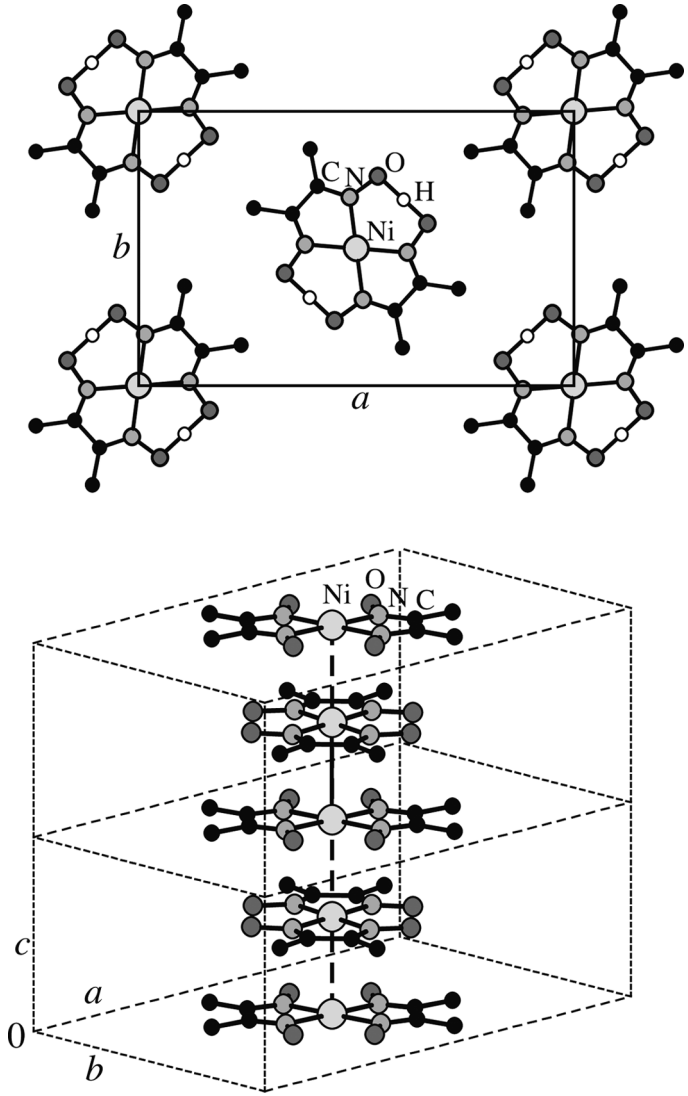

FIGURE 1 Crystal structure of Ni(dmg)$_2$.

EXPERIMENTAL

Ni(dmg)$_2$ was prepared from an aqueous solution of $NiCl_2$ and a hot alcoholic solution of dimethylglyoximes. This complex is characterized

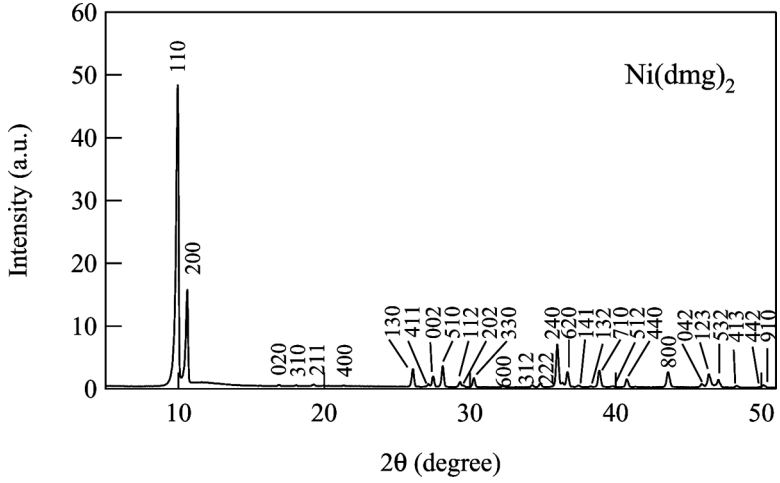

FIGURE 2 Powder X-ray diffraction pattern with CuK_α radiation for $Ni(dmg)_2$ at ambient pressure.

by powder X-ray diffraction using CuK_α radiation and silicon as a standard. Figure 2 shows a powder X-ray diffraction pattern of $Ni(dmg)_2$ at ambient pressure. All diffraction lines were indexed in the orthorhombic structure [8]. The values of the lattice constant obtained from powder X-ray diffraction lines for $Ni(dmg)_2$ agree with almost all results (Table 1) of the single-crystal diffraction data.

By use of synchrotron radiation, powder X-ray diffraction of $Ni(dmg)_2$ was studied with a diamond-anvil cell and an imaging plate at pressures up to 7.4 GPa at room temperature [5,6]. The incident beam

TABLE 1 Lattice Constant, Linear Compressibility (K_{0L}), and Bulk Compressibility (K_0) for $Ni(dmg)_2$, $Pt(dmg)_2$, and $Pt(dpg)_2$

Parameter	$Ni(dmg)_2$	$Pt(dmg)_2$	$Pt(dpg)_2$
a (Å)	16.68	16.7735	22.829
b (Å)	10.44	10.579	15.4591
c (Å)	6.49	6.5175	7.0114
d (g/cm^3)	1.70	2.443	1.809
K_{0a} (GPa^{-1})	0.0113(3)	0.0190(4)	0.0134(6)
K_{0b} (GPa^{-1})	0.02(2)	0.0158(7)	0.0075(6)
K_{0c} (GPa^{-1})	0.034(2)	0.0312(8)	0.040(2)
K_0 (GPa^{-1})	0.125	0.1	0.132

was monochromatized by Si(111) double crystals. The X-ray beam with a wavelength of $\lambda = 0.6199$ Å was collimated to 40 nm in diameter. High-pressure diffraction experiments were performed at the beam line (BL – 18 C) of the KEK Photon Factory in Tsukuba. A 4:1 methanol–ethanol solution was used as the hydrostatic pressure fluid. The pressure in a diamond-anvil cell was determined from a pressure shift in the sharp R-line fluorescence spectrum of ruby. The measurement of X-ray diffraction was carried out under hydrostatic conditions because the 4:1 methanol–ethanol solution used as pressure medium was solidified at around 10 GPa.

The absorption spectra of Ni(dmg)$_2$ were measured with the diamond-anvil cell up to 11 GPa at room temperature [2]. The optical system comprised a standard microscope and a spectrophotometer with an associated photodetection system. A FT-IR (Nicolet Magna-IR760) was used for the measurement of the absorption spectra in the near infrared region. A thin film of this complex was prepared by evaporation onto the surface of the diamond-anvil in high vacuum. The thickness of the evaporated film is about 1500 Å. Fluorinert was used as the hydrostatic pressure fluid. The electrical resistivity of polycrystalline Ni(dmg)$_2$ was measured as a function of pressure up to 23 GPa at room temperature [9].

RESULTS

X-ray Study of Ni(dmg)$_2$ with Synchrotron Radiation at High Pressures

Figure 3 shows powder X-ray diffraction patterns measured with synchrotron radiation of $\lambda = 0.6197$ Å for Ni(dmg)$_2$ at high pressures. As shown in Fig. 2, two very strong diffraction lines, 110 and 200, of the complex are observed in the low-angle region. However, both strong lines are cut in Fig. 3 because there are many weak diffraction lines in the high-angle region. These diffraction lines shift to the high-angle region with increasing pressure. Each line shows the different pressure shift. The d-value of the 002 line agrees with the Ni–Ni distance in the linear metal chains. This line is very sensitive to pressure. The intensity of the diffraction lines decreases and the width broadens with increasing pressure. The change of the powder X-ray diffraction pattern with the phase transition for Ni(dmg)$_2$ is not observed up to 7.4 GPa. When pressure is reduced from 7.4 GPa to the ambient pressure, the diffraction pattern at normal pressure appears again at room temperature. This behavior is completely reversible.

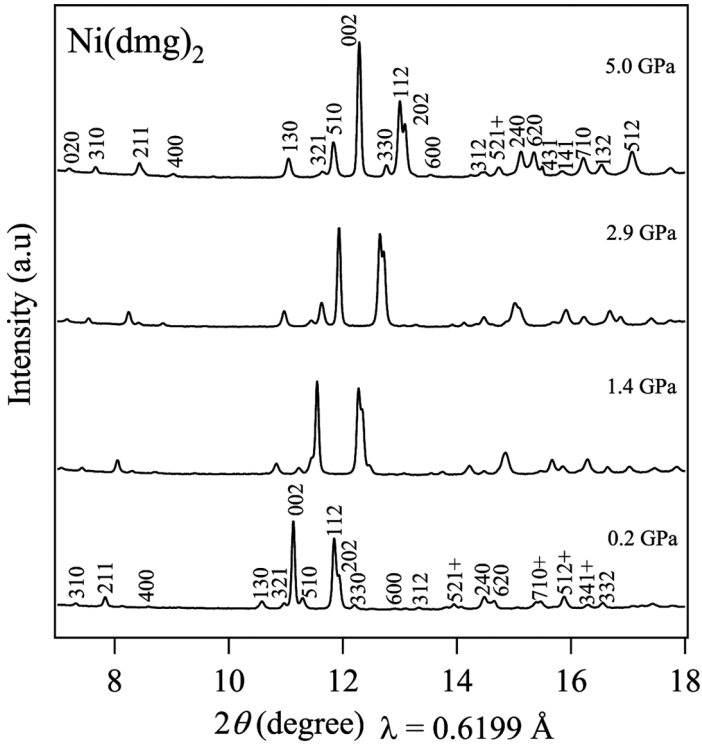

FIGURE 3 Powder X-ray diffraction patterns with synchrotron radiation for $Ni(dmg)_2$ at high pressures.

Figure 4 shows the ratio of lattice constant (L/L_0, where L_0 is the value at ambient pressure) versus pressure curves for $Ni(dmg)_2$. As shown in Fig. 1, the crystal structure of the complex is anisotropic. The lattice constant of each axis shows the different pressure dependence. These experimental data can be fitted by a quadratic equation of state:

$$\frac{L}{L_0} = 1 + K_{0L}P + K'_L P^2 \tag{1}$$

where K_{0L} is the linear compressibility of each axis, K'_L its pressure derivative, and P the pressure. The magnitude of the linear compressibility increases in the order $c > b > a$ in the low-pressure region. However, the lattice constant along the b-axis tends to level at pressures greater than 4 GPa. The lattice constants along a- and b-axes

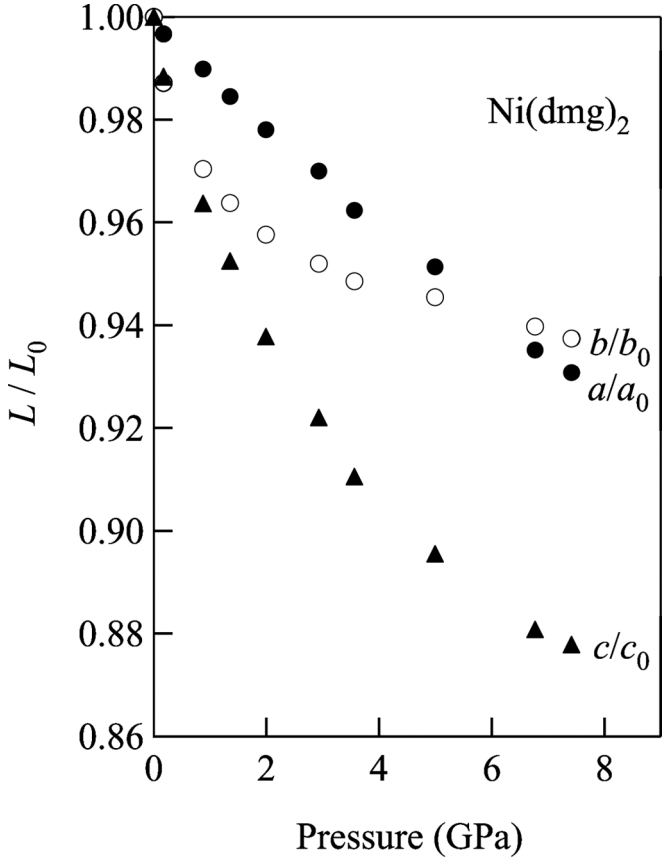

FIGURE 4 Ratio of lattice constant (L/L_0) versus pressure curves for Ni(dmg)$_2$ at room temperature.

are not sensitive to pressure compared with that along the *c*-axis. On the other hand, the *c*-axis is very compressible. We have already studied powder X-ray diffraction of Pt(dmg)$_2$ with synchrotron radiation at high pressures [4]. The values of the lattice constant and the linear compressibility for Ni(dmg)$_2$, Pt(dmg)$_2$, and Pt(dpg)$_2$ are summarized in Table 1. The *c*- and *b*-axes of Ni(dmg)$_2$ are more shrinkable than those of Pt(dmg)$_2$. In contrast, the *a*-axis of Ni(dmg)$_2$ is less compressible compared with that of Pt(dmg)$_2$.

Figure 5 shows the relative cell volume (V/V_0) versus pressure curve for Ni(dmg)$_2$. The cell volume monotonically decreases with increasing pressure up to 7.4 GPa. The experimental data can be fitted

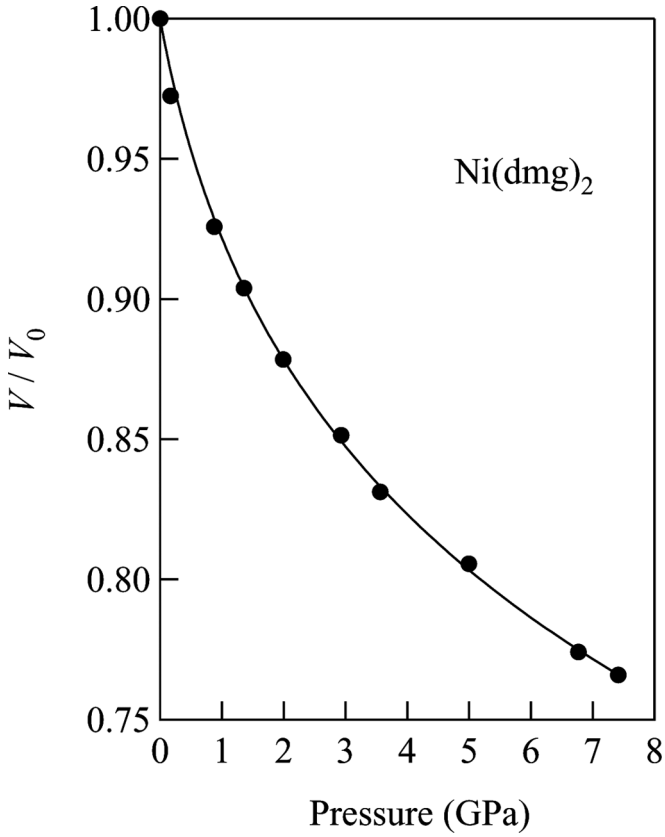

FIGURE 5 Relative cell volume (V/V_0) versus pressure curve for Ni(dmg)$_2$. The solid line is the fitted Birch equation of state.

by a Birch equation of state [13]:

$$P = \left(\frac{3}{2}\right)B_0\left[\left(\frac{V}{V_0}\right)^{-7/3} - \left(\frac{V}{V_0}\right)^{-5/3}\right] \times \left\{1 - \frac{3}{4}(4 - B_0')\left[\left(\frac{V}{V_0}\right)^{-2/3} - 1\right]\right\} \quad (2)$$

where B_0 is the bulk modulus, B_0' its first pressure derivative, V the volume, and P the pressure. A least-squares fit to the data of Ni(dmg)$_2$ gives the following values: $B_0 = 8.0 \pm 0.4$ GPa and $B_0' = 11.0 \pm 0.7$. The bulk modulus is defined as follows: $B_0 = -V_0\ \mathrm{d}P/\mathrm{d}V$. The bulk compressibility (K_0) is $K_0 = 1/B_0$. The bulk modulus and its pressure

derivative of Pt(dmg)$_2$ are $B_0 = 10.0 \pm 0.5$ GPa, $B_0' = 7.2 \pm 0.5$, respectively. The bulk modulus of Ni(dmg)$_2$ is smaller than that of Pt(dmg)$_2$. Ni(dmg)$_2$ is somewhat compressible compared with Pt(dmg)$_2$.

Absorption Spectra and Electrical Resistivity of Ni(dmg)$_2$ at High Pressures

Absorption bands of the thin film of Ni(dmg)$_2$ are observed at around 410 and 530 nm at ambient pressure. The 410-nm band is ascribed to the metal-to-ligand charge-transfer ($d\pi$–π^*) transition, and the 530-nm band is due to the $3d_z^2$–$4p_z$ transition in the central metal [10]. Figure 6 shows absorption spectra of the thin film of Ni(dmg)$_2$ at

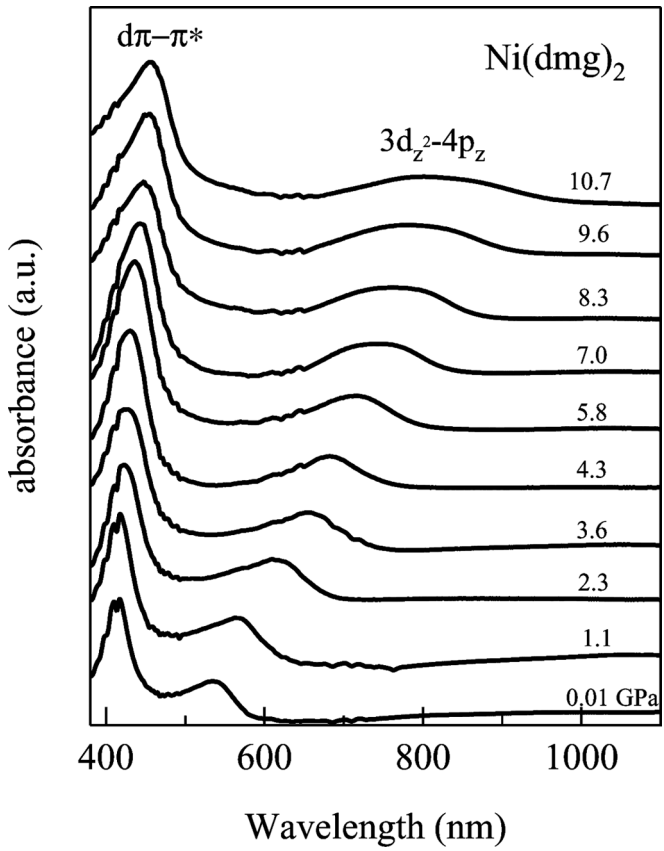

FIGURE 6 Effect of the pressure on the absorption spectra of the thin film of Ni(dmg)$_2$.

high pressures. We have studied the absorption band in detail in the near-infrared region at higher pressures. The $d\pi$–π^* and 3d–4p bands in the visible region monotonously shift to the lower energy region up to 11 GPa. Figure 7 shows the pressure shift of the absorption peaks for both bands in $Ni(dmg)_2$. The average pressure shift of the d–p band is much larger than that of the $d\pi$–π^* band. The peak of the d–p band shifts from 18, 900 cm^{-1} at ambient pressure to 12, 400 cm^{-1} at 10.7 GPa. The rate of the average pressure shift is about $-600\ cm^{-1}$/GPa. The absorption edge of $Ni(dmg)_2$ is located at around 17, 100 cm^{-1} (585 nm) at normal pressure. From Fig. 7, the pressure in which the optical energy gap between $3d_z^2$ and $4p_z$ bands becomes zero is expected to be greater than 28 GPa. In contrast, the absorption edge of the 5d–6p transition in $Pt(dmg)_2$ is observed at around

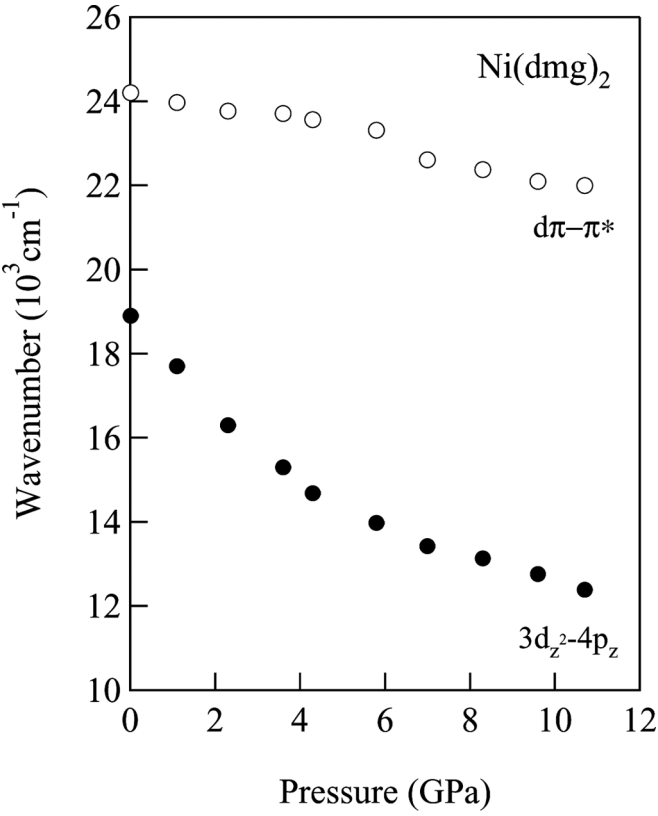

FIGURE 7 Absorption peak energy versus pressure curves for $d\pi$–π^* and 3d–4p bands in $Ni(dmg)_2$.

12,000 cm^{-1} at ambient pressure. A rate of the average shift of this band is -2300 cm^{-1}/GPa [2]. Thus, the optical energy gap between $5d_z{}^2$ and $6p_z$ bands for Pt(dmg)$_2$ becomes zero at around 5 GPa. Figure 8 shows the peak energy versus M–M distance curves for Ni(dmg)$_2$ and Pt(dmg)$_2$. The peak energies of both complexes decrease linearly with decreasing M–M distances. However, the slope of Pt(dmg)$_2$ is much larger than that of Ni(dmg)$_2$. The Pt–Pt distance within the chain becomes less than 2.9 Å at around 5.0 GPa. This distance almost agrees with the Pt–Pt spacing of the one-dimensional metal, $K_2Pt(CN)_4Br_{0.3}3H_2O$. The M–M distances along the linear chains for Ni(dmg)$_2$ and Pt(dmg)$_2$ are almost the same at high pressures. However, the pressure shift of the d–p band for both complexes differs remarkably. Further, the new pressure-induced absorption band

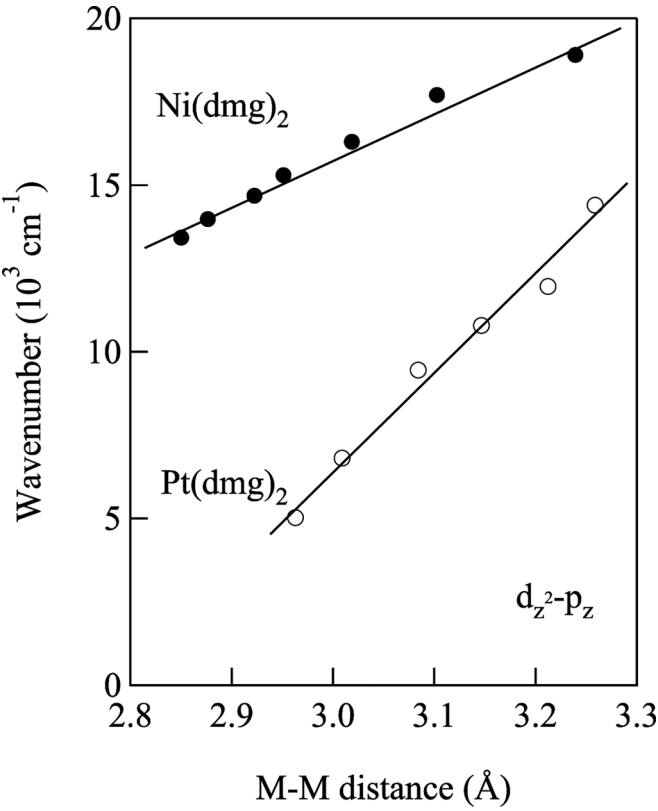

FIGURE 8 Absorption peak energies plotted as a function of the M–M distance for Ni(dmg)$_2$ and Pt(dmg)$_2$.

for $Pt(dmg)_2$ has been observed at around 540 nm above 6.2 GPa [14]. Thus, the electronic states of $Ni(dmg)_2$ and $Pt(dmg)_2$ differ essentially at higher pressures.

Figure 9 shows the resistivity of polycrystals of $Ni(dmg)_2$ and $Pt(dmg)_2$ at high pressures. The resistivity of $Ni(dmg)_2$ decreases monotonically with increasing pressure up to 23 GPa. The lowest resistivity of this complex is about 50 Ωcm at around 23 GPa. On the other hand, the resistivity of $Pt(dmg)_2$ drastically decreases with increasing pressure, reaches the minimum at around 6.5 GPa, and then slowly increases with increasing pressure greater than this pressure. The lowest resistivity of this complex is 0.1 Ω cm at around 6.5 GPa. The electrical behavior of both complexes is very different at high pressures.

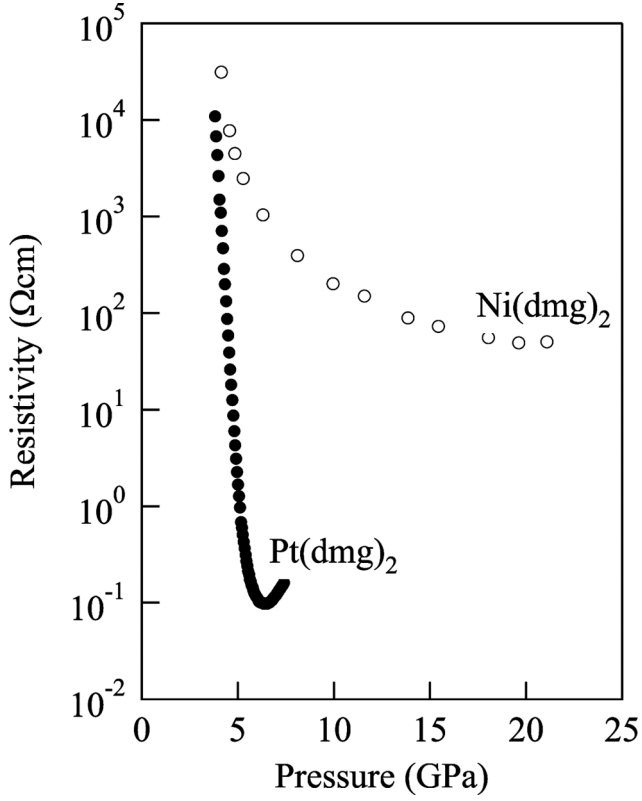

FIGURE 9 Electrical resistivity of $Ni(dmg)_2$ and $Pt(dmg)_2$ at high pressures.

DISCUSSION

A molecule of Ni(dmg)$_2$ is a d^8-square planar complex; each Ni^{2+} ion is surrounded by four nitrogen atoms of two dimethylglyoxime anions. The 3d orbitals of a Ni^{2+} ion are split into four energy levels (d_{xy}, d_z^2, d_{yz} and d_{zx}, $d_x^2 - {}_y^2$) by a crystal field of D_{4h} symmetry, where d_{yz} and d_{zx} are double degeneracy. The eight d electrons of the Ni^{2+} ion core fill the d_z^2, d_{yz}, d_{zx}, and $d_x^2 - {}_y^2$ states [1,10,12]. The complex crystallizes in columnar structures. The columns are formed by square planar complex molecules with the relatively short Ni–Ni distance of 3.255 Å in a direction of the stacks. The overlap of the $3d_z^2$ orbitals can be produced a valence band that is completely filled by 8d electrons. The conduction band is composed of $4p_z$ orbitals. Both bands are separated by large energy gap at normal pressure. The band structure of Pt(dmg)$_2$ is similar to that of Ni(dmg)$_2$ at ambient pressure [1].

The lowest resistivity of Ni(dmg)$_2$ is about 50 Ω cm at around 23 GPa. The pressure in which the optical energy gap between $3d_z^2$ and $4p_z$ bands becomes zero is greater than 28 GPa. Thus, Ni(dmg)$_2$ shows the semiconducting behavior even at very high pressures. On the other hand, the resistivity of Pt(dmg)$_2$ drastically decreases with increasing pressure up to 6.5 GPa, and then reaches the resistivity minimum. The energy gap of this complex rapidly decreases with decreasing Pt–Pt distance, becoming zero at around 5 GPa. Then, the $6p_z$ conduction band crosses the $5d_z^2$ valence band at around 5 GPa. The insulator-to-metal transition is observed at around this pressure [2]. Electrical and optical behaviors of Ni(dmg)$_2$ and Pt(dmg)$_2$ are very different at high pressures though the bulk and linear compressibilities for both complexes are almost same. These may mainly be explained in terms of the relative spatial extent of the outer d and p orbitals in Ni and Pt atoms.

At pressures greater than 6.5 GPa, the resistivity of Pt(dmg)$_2$ slowly increases with increasing pressure. Pt(dmg)$_2$ behaves as the insulator again at around 6.5 GPa. The Pt–Pt distance monotonously decreases with increasing pressure even greater than 6.5 GPa. Because the width of the $5d_z^2$ and $6p_z$ bands must widen with increasing pressure, the metallic phase should be stabilized at higher pressures. However, Pt(dmg)$_2$ changes from the metal to the insulator at 6.5 GPa. This result suggests that the electrical behavior of Pt(dmg)$_2$ cannot be explained by the model of two bands ($5d_z^2$ and $6p_z$) at pressures greater than the pressure that shows the resistivity minimum. Further, the new absorption band for Pt(dmg)$_2$ is induced at around 540 nm under 6.5 GPa [14].

Bella et al. have studied the molecular orbitals of a Pt(dmg)$_2$ molecule by ab initio linear-combination-of-atomic-orbitals self-consistent-field

(LCAO-MO SCF) calculations [15]. The top of the valence band consists of the $9a_g$ molecular orbital (d_z^2 character, metal-based molecular orbital) at ambient pressure. There is the $3b_{3g}$ orbital (d_{yz} and π_4 character, ligand-based molecular orbital) below the energy level of the $9a_g$ orbital. As mentioned previously, the resistivity minimum and the metal-to-insulator transition for $Pt(dmg)_2$ are observed at around 6.5 GPa. These arise from essentially the change of the electronic states. We have suggested that the highest-occupied-molecular-orbital (HOMO) of $Pt(dmg)_2$ is replaced from the metal-based orbital to the ligand-based orbital at higher pressures [2].

The linear and bulk compressibilities for $Ni(dmg)_2$ and $Pt(dmg)_2$ are almost same. However, the resistivity of $Ni(dmg)_2$ decreases monotonically with increasing pressure greater than 6 GPa. The pressure-induced absorption band for $Ni(dmg)_2$ is not found up to 30 GPa [11]. We suggest that the band structure of $Ni(dmg)_2$ differs essentially that of $Pt(dmg)_2$ at high pressures.

ACKNOWLEDGMENTS

This work was partly supported by Grants-in-Aid for Scientific Research from the Ministry of Education, Culture, Sports, Science and Technology of Japan: Nos. 17750186 (K. T.) and 17540310 (I. S.).

REFERENCES

[1] Shirotani, I., Kawamura, A., Suzuki, K., Utsumi, W., & Yagi, T. (1991). *Bull. Chem. Soc. Jpn.*, *64*, 1607–1612.
[2] Takeda, K., Shirotani, I., & Yakushi, K. (2000). *Chem. Mater.*, *12*, 912–916.
[3] Takeda, K., Shirotani, I., Sekine, C., & Yakushi, K. (2000). *J. Phys. Condens. Matter*, *12*, L483–L488.
[4] Takeda, K., Shirotani, I., & Yakushi, K. (2003). *Synthetic Metals*, *133–134*, 415–416.
[5] Shirotani, I., Hayashi, J., & Takeda, K. (2005). *Mol. Cryst. Liq. Cryst.*, *442*, 145–154.
[6] Takeda, K., Hayashi, J., Shirotani, I., Fukuda, H., & Ito, K. (2006). *Mol. Cryst. Liq. Cryst.*, *452*, 113–122.
[7] Takeda, K., Shirotani, I., Yakushi, K., & Yamashita, M. (2000). In: *Science and Technology of High Pressure (Proceedings of AIRAPT-17)*, Manghnani, M. H., Nellis, W. J., & Nicol, M. F. (Eds.), Universities Press: Hyderabad, India, Vol. 2, 998–1001.
[8] Godycki, L. E. & Rundle, R. E. (1953). *Acta Crystallogr.*, *6*, 487–494.
[9] Shirotani, I., Onodera, A., & Hara, Y. (1981). *J. Solid State Chem.*, *40*, 180–188.
[10] Ohashi, Y., Hanazaki, I., & Nagakura, S. (1970). *Inorg. Chem.*, *9*, 2551–2556.
[11] Takacz, K. & Drickamer, H. G. (1986). *J. Chem. Phys.*, *85*, 1184–1189.
[12] Shirotani, I., Suzuki, K., Suzuki, T., Yagi, T., & Tanaka, M. (1992). *Bull. Chem. Soc. Jpn.*, *65*, 1078–1083.
[13] Birch, F. (1947). *Phys. Rev.*, *71*, 809–814.
[14] Shirotani, I. & Suzuki, T. (1986). *Solid State Commun.*, *59*, 533–535.
[15] Bella, S. D., Casarin, M., Fragala, I., Granozzi, G., & Marks, T. J. (1988). *Inorg. Chem.*, *27*, 3993–4002.